Proceedings of IMECE2007
2007 ASME International Mechanical Engineering Congress and Exposition
November 11-15, 2007, Seattle, Washington, USA

IMECE2007-41348

THE DESIGN SPACE OF SUPERALLOY-BASED ACTIVELY COOLED COMBUSTOR WALLS FOR H_2-POWERED HYPERSONIC VEHICLES

Lorenzo Valdevit
Mechanical and Aerospace Engineering Department
University of California, Irvine
Irvine, CA 92697-3975
valdevit@uci.edu

Natasha Vermaak
Materials Department
University of California, Santa Barbara
Santa Barbara, CA 93106-5050
natasha@engineering.ucsb.edu

Frank W. Zok
Materials Department
University of California, Santa Barbara
Santa Barbara, CA 93106-5050
zok@engineering.ucsb.edu

A. G. Evans
Materials Department
University of California, Santa Barbara
Santa Barbara, CA 93106-5050
agevans@engineering.ucsb.edu

ABSTRACT

The walls of combustion chambers used for air-breathing hypersonic vehicles are subject to substantial thermo-mechanical loads, and require active cooling by the fuel in conjunction with advanced material systems. Solutions based on metallics are preferable to ceramic matrix composites due to their lower cost and greater structural robustness. Previous work suggested that a number of metallic materials (e.g. Nickel, Copper and Niobium alloys) could be used to fabricate actively cooled sandwich structures that withstand the thermo-mechanical loads for a Mach 7, hydrocarbon-powered vehicle (albeit with different weight efficiencies). However, this conclusion changes when the Mach number is increased. This work explores the feasibility of the Nickel superalloy MAR-M246 for a wide range of Mach numbers (7-12). Since hydrocarbon fuels are limited to Mach 7-8, Hydrogen is used as the coolant of choice. A previously derived analytical model (appropriately modified for gaseous coolant) is used to explore the design space. The relative importance of each design constraint is assessed, resulting in the distillation of essential guidelines for optimal design.

NOMENCLATURE

A	=	area [m^2]
a	=	speed of sound [m/s]
b	=	width of the actively cooled panel [m]
c_p	=	specific heat [J/kg K]
C_μ	=	coefficient in the visc./temp. relation [K]
C_k	=	coefficient in the cond./temp. relation [K]
D	=	diameter [m]
E	=	Young's modulus [Pa]
f	=	friction factor
H	=	thickness of the actively cooled panel [m]
h	=	heat transfer coefficient [W/m^2K]
k	=	thermal conductivity [W/m K]
L	=	height of the cooling channel [m]
$\dot{m}$	=	mass flow rate [kg/s]
Ma	=	Mach number
Nu	=	Nusselt number
p	=	pressure [Pa]
Pr	=	Prandtl number
q	=	specific heat flux [W/m^2]
R	=	universal gas constant [J/kg K]
	=	thermal resistance per unit width [$(W/m\ K)^{-1}$]
r	=	thermal resistance per unit area [$(W/m^2K)^{-1}$]
Re	=	Reynolds number
T	=	temperature [K]
t	=	thickness [m]
u	=	velocity of the coolant [m/s]
w	=	width of the cooling channel [m]
x,y,z	=	spatial coordinate [m]
Z	=	length of the actively cooled panel [m]

Greek symbols

α	=	thermal expansion coefficient (CTE) [K^{-1}]
	=	non-dimensional parameter
β	=	non-dimensional parameter
γ	=	non-dimensional parameter
Δ	=	difference
μ	=	dynamic viscosity [Pa s]
ν	=	Poisson's ratio
Π	=	constraint activity parameter
ρ	=	mass density [kg/m^3]
$\bar{\rho}$	=	areal density of the cross-section of the panel
σ	=	normal stress [Pa]
θ	=	fin temperature: $T(y) - T_{fuel}$ [K]

Subscripts and superscripts

0	=	inlet conditions
	=	reference value
1,2	=	generic symbols
c, core	=	relative to the core web
c, cool	=	relative to the cooling channels
f, face	=	relative to the face sheet
f, fuel	=	relative to the fuel (coolant)
fin	=	relative to conduction/convection in the core web
G	=	relative to the hot gases in the combustion chamber
h	=	hydraulic
	=	horizontal (x) direction
i	=	generic location in the cross-section
m	=	mechanical
max	=	maximum
min	=	minimum
panel	=	relative to the whole cross-section of the panel
s	=	relative to the solid material the panel is made of
T	=	thermal
ft	=	top side of the top face
fb	=	bottom side of the top face
w	=	between core webs (i.e. near the middle of the channel)
x,y,z	=	along the respective directions
Y	=	yielding
ΔT_{panel}	=	due to the temperature drop across the panel
ΔT_{tf}	=	due to the temperature drop across the top face sheet
*	=	generic symbol

1. INTRODUCTION

The potential of air-breathing hypersonic vehicles for space access and military applications has been clearly demonstrated. Although the fundamental aerodynamics and the feasibility of stable supersonic combustion have been studied in detail, the integration with vehicle design remains a challenge. Among the most daunting tasks is the development of materials and structures that withstand the enormous thermo-mechanical loads in severe environments. The walls of the combustion chamber and the leading edges of the vehicle are the most critical surfaces. This paper discusses metallic sandwich panels, actively cooled by the fuel, as thermo-structural solutions for combustion chamber walls.

An optimal design code that enables ranking of materials on the basis of weight efficiency has already been presented, and results have been derived for Mach 7, hydrocarbon-powered vehicles [1]. In this work we plan to extend those results to higher Mach numbers. Since hydrocarbon is not realistic for Mach >7-8, hydrogen is assumed as the fuel (and hence the coolant) of choice.

The overarching goal is the extraction of design guidelines that allow the selection of the optimal material and structure for a wide range of Mach numbers. A necessary step is the ability to predict with confidence the thermo-mechanical loads as a function of the Mach number of the vehicle. Unfortunately, this is not trivial, because of the complex aerothermodynamics in the combustion chamber, and the influence of the details of the vehicle design (e.g. shape, size and numbers of injectors, possible by-pass solutions, etc…).

In this work, we take a more fundamental approach. We investigate the design space of combustor liners made of Nickel superalloy (MAR-M246, see Table 1 for properties), for a wide range of thermo-mechanical loads and coolant flow rates. A previously derived analytical approach for the calculation of temperatures and stresses in the panel is modified to account for the compressibility of the coolant (section 2). For every choice of the external loads (here envisioned as input parameters), the geometry of the panel is optimized on the base of weight-efficiency, subject to a number of design constraints (section 3). When the optimization code fails to converge to a solution, the combination of input parameter is considered external to the design space. This allows the construction of design maps (section 4). Investigation of the optimal designs for a specific value of the heat flux ($q_G = 3MW/m^2$) allows a clear understanding of the effect of coolant flow rate and internal pressure (section 5). Conclusions and future work follow.

2. THE THERMO-MECHANICAL MODEL

This section presents an analytical model for the calculation of temperature and stress distributions in an actively cooled panel (Fig. 1) under uniform flux boundary conditions. Assumptions leading to realistic estimates of heat fluxes and coolant pressures are presented elsewhere [2]. The coolant is assumed gaseous (hydrogen), and the dependence of its physical properties on temperature and pressure is addressed.

Section A presents the thermal network model used to calculate the temperatures in the solid at a number of discrete points, at any given cross section. Stress calculation is presented in Section B.

A. Temperature distribution

To facilitate the derivation of analytic estimates for the temperatures, three simplifications are invoked:

(i) The top face of the structure is subjected to a uniform heat flux, q_G, whereas the bottom face and the sides are thermally insulated. Consequently, all the heat received through the top face is carried away by the cooling fluid.

(ii) No heat is conducted along the length of the panel (z-direction), either in the structure or in the cooling fluid. This assumption results in slightly conservative temperature estimates.

(iii) The fuel temperature is uniform within the channels at any given cross-section: $T_{fuel} = T_{fuel}(z)$ only. Namely, T_{fuel} is the mixing-cup temperature.

The temperature at every cross-section *z* is calculated using an electrical analogy (Fig. 2a). Five thermal resistances (per unit length in the z-direction) are needed to characterize the problem (refer to Fig. 1b and the nomenclature for definition of the geometric variables):

• Conductive resistance across the face (y-direction): $R_{face} = t_f / k_s t_c$, $R^w_{face} = t_f / k_s w$

• Conductive resistance along the face (x-direction)[1]: $R_h = \left(w + t_c / 2\right) / 4 k_s t_f$

• Convective resistance on the coolant side (for the portion of the face in direct contact with the coolant): $R_{cool} = 1 / h_c w$

• Combined conductive and convective resistance of the core web (modeled as a one-dimensional thermal fin [3, 4]): $R_{fin} = \left\{\tanh^{-1}\left(\sqrt{\frac{2h_c}{k_s t_c}L^2}\right)\right\}\frac{1}{t_c}\left[\sqrt{\frac{2h_c}{k_s t_c}}k_s\right]^{-1}$.

Here, h_c is the heat transfer coefficients on the coolant side, and k_s is the thermal conductivities of the solid material. Flow in the cooling ducts is assumed to be turbulent and fully developed. Under these conditions, h_c is given by the correlation [5, 6]:

$$h_c = \frac{k_f}{D_h} Nu = \frac{k_f}{D_h}\frac{(f/2)(\mathrm{Re}-1000)\,\mathrm{Pr}}{1+12.7\sqrt{f/2}\left(\mathrm{Pr}^{2/3}-1\right)} \qquad (1)$$

where k_f is the thermal conductivity of the coolant, Pr is the Prandtl number, $D_h = 2wL/(w+L)$ is the hydraulic diameter of the ducts, and Re is the Reynolds number in the ducts, defined as:

$$\mathrm{Re} \equiv \frac{\rho_f u D_h}{\mu_f} = \frac{\dot{m}}{\mu_f\left(1-\bar{\rho}\right)}\frac{D_h}{bH} \qquad (2)$$

with μ_f being the dynamic viscosity of the fluid, $\dot{m}$ the prescribed mass flow rate of the fuel, $\bar{\rho} = 1 - Lw/(H(w+t_c))$ the areal density of the cross-section and *f* the friction factor. For fully developed turbulent flow in the range $2\cdot 10^4 < \mathrm{Re} < 10^6$, the following correlation can be used for the friction factor [5, 7]:

$$f = 0.046\,\mathrm{Re}^{-1/5} \qquad (3)$$

Eqs. (1)-(3) allow calculation of the thermal resistances R_{cool} and R_{fin} as a function of the geometric variables, the fuel properties, and flow rate.

If we assume that the specific heat of the coolant, $c_{p,f}$, is not a strong function of temperature (Table 2), then the temperatures of the fluid increases linearly along the *z*-direction, becoming maximum at the outlet. A simple energy balance yields:

$$T_{fuel}\left(z\right) = T_{f0} + \frac{q_G b}{\dot{m} c_{p,f}} z \qquad (4)$$

For reasonable values of the parameters, the coolant temperature varies considerably over the length of the panel. Hence, variations in density, viscosity and conductivity (and consequently in friction factor (Eq. (3)) and heat transfer coefficient (Eq. (1)) cannot be neglected. The implication is that the temperature in the solid is *not* linear in *z*.

The model can be simplified into the effective network of Fig. 2b, characterized by the five resistances $R^w_1, R^c_1, R^w_2, R^c_2, R_h$, where:

$$\begin{aligned} R^w_1 &= R^w_{face}/2 \\ R^c_1 &= R_{face}/2 \\ R^w_2 &= R^w_{face}/2 + R_{cool} \\ R^c_2 &= R_{face}/2 + R_{fin} \end{aligned} \qquad (5)$$

The unknowns are the temperatures at the top side of the top face, above the web and away from it (T^c_{ft} and T^w_{ft}, respectively), the corresponding temperatures at the middle of the top face (T^c_{fm} and T^w_{fm}, respectively) and the horizontal heat flux, q_h. Five equations are needed to close the system:

[1] The horizontal resistance is not properly conductive, as convection occurs along one of the sides: finite elements analyses revealed that using an effective length equal to half the physical length yields accurate results (hence the factor 4).

$$\begin{cases} T_{ft}^{c} - T_{fuel} = q_G r_1 + (q_G - 2q_h\, t_f / t_c)\, r_2^{c} \\ T_{ft}^{w} - T_{fuel} = q_G r_1 + (q_G + 2q_h\, t_f / w)\, r_2^{w} \\ T_{ft}^{c} - T_{fm}^{c} = q_G r_1 \\ T_{ft}^{w} - T_{fm}^{w} = q_G r_1 \\ T_{fm}^{c} - T_{fm}^{w} = q_h r_h \end{cases} \tag{6}$$

where the thermal resistances per unit area have been defined as:

$$\begin{aligned} r_1 &= \frac{1}{2}\frac{t_f}{k_s} \\ r_2^{w} &= \frac{1}{2}\frac{t_f}{k_s} + \frac{1}{h_c} \\ r_2^{c} &= \frac{1}{2}\frac{t_f}{k_s} + r_{fin} \\ r_{fin} &= \left\{ \tanh^{-1}\left(\sqrt{\frac{2h_c}{k_s t_c}}\, L^2 \right) \right\} \left[\sqrt{\frac{2h_c}{k_s t_c}}\, k_s \right]^{-1} \\ r_h &= \frac{\left(w + t_c / 2 \right) / 2}{k_s} \end{aligned} \tag{7}$$

Solving the linear system in Eq. (6), gives:

$$\begin{aligned} T_{ft}^{c} - T_{fuel} &= q_G r_1 \left(1 + \alpha\; r_2^{c} / r_1 \right) \\ T_{ft}^{w} - T_{fuel} &= q_G r_1 \left(1 + \beta\; r_2^{w} / r_1 \right) \\ T_{fm}^{c} - T_{fuel} &= q_G \alpha\; r_2^{c} \\ T_{fm}^{w} - T_{fuel} &= q_G \beta\; r_2^{w} \\ q_h &= \gamma\, q_G \end{aligned} \tag{8}$$

where α, β and γ are non-dimensional parameters given by:

$$\begin{aligned} \alpha &= \frac{r_h + 2 r_2^{w} \left(t_f / t_c + t_f / w \right)}{r_h + 2\, r_2^{c}\, t_f / t_c + 2\, r_2^{w}\, t_f / w} \\ \beta &= \frac{r_h + 2 r_2^{c} \left(t_f / t_c + t_f / w \right)}{r_h + 2\, r_2^{c}\, t_f / t_c + 2\, r_2^{w}\, t_f / w} \\ \gamma &= \frac{r_2^{c} - r_2^{w}}{r_h + 2\, r_2^{c}\, t_f / t_c + 2\, r_2^{w}\, t_f / w} \end{aligned} \tag{9}$$

Notice that Eq. (8) holds at any cross-section. Since r_2^{w} and r_2^{c} depend on the coolant temperature, though, the temperature at every point in the solid does *not* have the same *z*-variation as the mixing-cup temperature of the fuel.

For the calculation of the thermal stresses, two temperature differences are relevant:

(i) the temperature drop across the top face (in the y-direction), both over and between the core webs:

$$\begin{aligned} \Delta T_f^{c} &= 2\; q_G r_1\, \gamma\, \frac{t_f}{t_c} \\ \Delta T_f^{w} &= 2\; q_G r_1 \left(1 + \gamma\, \frac{t_f}{w} \right) \end{aligned} \tag{10}$$

(ii) the temperature drop across the entire panel cross section, measured from the middle of the top face to the bottom face (the bottom face is assumed to be isothermal and at the same temperature as the bottom end of the core web), both over and between the core webs:

$$\begin{aligned} \Delta T_{panel}^{c} &= q_G r_1 \left(1 - 2\gamma\, \frac{t_f}{t_c} \right) \left[1 + \frac{r_{fin}}{r_1} \left(1 - \frac{\theta(L)}{\theta_0} \right) \right] \\ \Delta T_{panel}^{w} &= q_G r_1 \left[\left(1 + 2\gamma\, \frac{t_f}{w} \right) \frac{r_2^{w}}{r_1} - \frac{\theta(L)}{\theta_0} \left(1 - 2\gamma\, \frac{t_f}{t_c} \right) \frac{r_{fin}}{r_1} \right] \end{aligned} \tag{11}$$

Here, $\theta(y)/\theta_0$ is the non-dimensional fin temperature, namely:

$$\frac{\theta(y)}{\theta_0} = \frac{T(y) - T_{fuel}}{T(0) - T_{fuel}} = \frac{\cosh\left[\sqrt{\frac{2h_c}{k_s t_c}} \left(L - y \right) \right]}{\cosh\left[\sqrt{\frac{2h_c}{k_s t_c}}\, L \right]} \tag{12}$$

and *y* is the coordinate oriented along the fin.

B. Stress Distributions

Problem statement and boundary conditions

The thermo-mechanical stresses depend on the constraint exerted on the plate by the surrounding components of the vehicle. We assume that the bending effects due to the pressure in the combustion chambers can be eliminated by appropriately supporting the panel along the back face [1]. This results in the idealized boundary conditions of Fig. 3a. Uniform thermal expansion (but no panel-level bending) is permitted along either direction. The external pressure does not cause the panel to bend globally, but the internal pressure can bend individual top face segments. The use of rollers instead of frictional supports allows uniform thermal expansion of the panel (with no bending).

To further simplify the problem, both the pressure drop and the temperature variation along the panel length are neglected. This assumption, combined with the imposed boundary conditions, ensure that generalized plane strain conditions are attained along the *z* direction[2]. Furthermore, it requires that the calculations be performed on one cross-section only. Because the properties of the coolant are affected by temperature, the temperature differences that drive the thermal stresses (Eqs. (10)-(11)) vary with *z*. Concomitantly, the yield strength of the metal decreases with increasing temperature, indicating potential failure at the outlet. The implication is that a number of cross-sections should be analyzed for potential failure to guarantee conservative results.

The next step is the identification of the most failure-susceptible locations in the structure at each cross-section. The stresses due to both pressure and thermal loads vary along the member lengths and thicknesses, but are periodic in the width of the panel, *b* (i.e. they are the same at each cell). Because the thermal and pressure loads often induce stresses of opposite sign, it is not straightforward to establish *a priori* the location of first yield. For this reason, a set of 9 "critical points" has been identified (Fig. 3b). The presence of internal pressure in the core channels (which imposes significant tensile stresses on all members) combined with the relatively stubby shape of the optimized members makes it unnecessary to design against buckling [8-16]. Consequently, failure of the structure is averted provided that the Mises stress in the most critical location remains in the elastic range.

The analytic methods used to determine the stresses in sandwich structures consider the face and core members in each unit cell as independent beams; the connection between members is modeled using translational (and some degree of rotational) constraints [8-16]. The accuracy of this approach is dependent upon the aspect ratio of each element, and decreases as the elements become stubbier. When this approach is used, finite element analyses are needed to ensure that predictions at the optimal geometries are sufficiently accurate.

Stresses due to coolant pressure

The pressure p_{cool} inside the cooling channels subjects the core members to uniform tension and induces a combination of tension and bending on the faces. Using the notation of Figs. 1b and 3b, the resulting stresses in the core members (point 9) are:

$$\frac{\sigma_{core,y}^{p_{cool}}}{p_{cool}} = \frac{w}{t_c} \qquad \frac{\sigma_{core,z}^{p_{cool}}}{p_{cool}} = \nu \frac{\sigma_{core,y}^{p_{cool}}}{p_{cool}} \tag{13}$$

and in the face segments:

$$\frac{\sigma_{face,x}^{p_{cool}}}{p_{cool}} = \begin{cases} L/2t_f - \left(w/t_f\right)^2/2 & \text{at pt 1} \\ L/2t_f + \left(w/t_f\right)^2/2 & \text{at pt 2} \\ L/2t_f + \left(w/t_f\right)^2/4 & \text{at pt 5} \\ L/2t_f - \left(w/t_f\right)^2/4 & \text{at pt 6} \\ L/2t_f & \text{at pts } 3,4,7,8 \end{cases} \tag{14}$$

$$\frac{\sigma_{face,z}^{p_{cool}}}{p_{cool}} = \nu \frac{\sigma_{face,x}^{p_{cool}}}{p_{cool}}$$

Consistent with beam analysis, the through-thickness stresses are neglected.

Thermal stresses

At time zero the entire structure is at the same temperature as the fuel at the inlet, T_{f0}, and no thermal stresses are present. Upon exposure to the combusting gases, the temperature distribution reaches a steady state. Because the boundary conditions allow uniform expansion of the panel, the problem can be modeled by superimposing the stresses due to two temperature differences. *Contribution 1*. By ignoring x-variations, the average temperature difference between the top and bottom faces, $\Delta T_{panel} = \left(\Delta T_{panel}^{w} + \Delta T_{panel}^{c}\right)\Big/2$ causes the panel to deform uniformly in both the *x* and *z* directions, inducing compression in the top face and tension in the bottom face [17]. Note that it is not legitimate to ignore the core stretching stiffness in the z-direction, where the core behaves as a continuous plate. When the core and the bottom face are at the same temperature, the resulting stresses are:

$$\sigma_{face,x}^{\Delta T_{panel}} = \begin{cases} -\dfrac{E\alpha\Delta T_{panel}}{2\left(1-\nu\right)} & \text{at pts } 1,2,5,6 \\ \dfrac{E\alpha\Delta T_{panel}}{2\left(1-\nu\right)} & \text{at pts } 3,4,7,8 \end{cases}$$

$$\sigma_{face,z}^{\Delta T_{panel}} = \begin{cases} -\dfrac{E\alpha\Delta T_{panel}\left(A_f + A_c\right)}{\left(1-\nu\right)\left(2A_f + A_c\right)} & \text{at pts } 1,2,5,6 \\ \dfrac{E\alpha\Delta T_{panel}\,A_f}{\left(1-\nu\right)\left(2A_f + A_c\right)} & \text{at pts } 3,4,7,8 \end{cases} \tag{15}$$

where $A_f = t_f(w + t_c)$ and $A_c = (H - 2t_f)t_c$ are the cross-sectional areas of the face and the core in a unit cell, respectively. Note that neglecting the core stiffness (letting $A_c \to 0$ in Eq. (15)) results in a perfectly bi-axial state of stress

[2] Generalized plane strain refers to conditions wherein the cross-sections $z = 0$ and $z = Z$ are not allowed to rotate relative to each other (although they are free to translate).

in both faces. *Contribution 2*. By ignoring x-variations, the temperature difference across the top face thickness, $\Delta T_f = \Delta T_f^w$, causes the upper surface of the top face to experience compression and the lower surface to be in tension, giving:

$$\sigma_{face,x}^{\Delta T_{tf}} = \sigma_{face,z}^{\Delta T_{tf}} = \begin{cases} -\dfrac{E\,\alpha\,\Delta T_{tf}}{2(1-\nu)} & \text{at pts 1,5} \\ \dfrac{E\,\alpha\,\Delta T_{tf}}{2(1-\nu)} & \text{at pts 2,6} \end{cases} \tag{16}$$

3. CONSTRAINTS

For every choice of the input parameters (the coolant pressure, p_{cool}, mass flow rate, $\dot{m}$, inlet temperature, T_{f0}, and the incoming heat flux, q_G), designs are acceptable if three conditions are met:

(i) the thermo-mechanical stresses do not exceed the (temperature dependent) yield strength of the material;

(ii) the maximum temperature in the material is below a critical level (defined as the temperature at which the yield strength drops significantly);

(iii) the pressure difference necessary to overcome frictional dissipation in the cooling channels is within allowable limits.

Condition (i) is expressed in terms of Mises stress:

$$\max_{i=1\div 9}\left\{\left(\frac{\sigma_{m,x}^{(i)}}{\sigma_Y(T^{(i)})}+\frac{\sigma_{T,x}^{(i)}}{\sigma_Y(T^{(i)})}-\frac{\sigma_{m,z}^{(i)}}{\sigma_Y(T^{(i)})}-\frac{\sigma_{T,z}^{(i)}}{\sigma_Y(T^{(i)})}\right)^2+\right.$$
$$\left.+\left(\frac{\sigma_{m,x}^{(i)}}{\sigma_Y(T^{(i)})}+\frac{\sigma_{T,x}^{(i)}}{\sigma_Y(T^{(i)})}\right)^2+\left(\frac{\sigma_{m,z}^{(i)}}{\sigma_Y(T^{(i)})}+\frac{\sigma_{T,z}^{(i)}}{\sigma_Y(T^{(i)})}\right)^2\right\}\le 2 \tag{17}$$

Eq. (17) guarantees that the panel survives the combined application of thermal *and* mechanical stresses. It does not guarantee survivability after the application of thermal or mechanical stresses *independently*. To ensure conservativeness, two more conditions similar to Eq. (17) must also be imposed for these alternative scenarios.

Condition (ii) can be expressed as:

$$\max\left\{T_{ft}^w, T_{ft}^c\right\} \le T^* \tag{18}$$

where T^* is the temperature at which the yield strength of the material drops unacceptably (Table 1).

The pressure drop is not linear in *z*, since the properties of hydrogen (and consequently the coolant velocity) are a function of temperature (and hence of *z*). The total pressure drop over the length of the panel can be obtained by integration:

$$\Delta p = \int_0^Z \frac{2\rho_f(z)u^2(z)f(z)}{D_h}dz = \int_0^Z \frac{2\,\dot{m}^2 f(z)}{\rho_f(z)D_h H^2 b^2(1-\bar{\rho})^2}dz \tag{19}$$

where *f* is the friction factor (Eq. (3)), ρ_f is the density of the coolant (Table 2), $\bar{\rho}$ and Z the areal density and the length of the panel, respectively.

4. DESIGN MAPS

We want to explore the feasibility of actively cooled panels made of the Nickel superalloy MAR-M246 as combustor walls for hypersonic vehicles. In order to encompass a large range of Mach numbers, we define a parameter space for heat flux and coolant flow rate:

$$\begin{aligned} q_G &= 1-6 \text{ MW/m}^2 \\ \dot{m} &= 0.05-25 \text{ kg/s} \end{aligned} \tag{20}$$

Additionally, three different coolant pressures are considered: p_{cool} = 5, 10, 30 MPa. The inlet temperature of the coolant is $T_{f0} = 200$ K. The combustor (and hence the panel) is assumed to be 1m long (*Z = 1* m) and 30cm wide (*b = 30* cm). Notice that the results apply to any width, provided that the flow rate be appropriately scaled. Also note that $\dot{m}$ is the flow rate into *one* panel. If all the four walls of the combustor are cooled simultaneously, this value will be 2-3 times smaller than the overall flow rate at the injectors. Again, with appropriate scaling of the flow rate the results apply to any configuration. The geometry of the panel is required to lie within the following space:

$$\begin{aligned} L &= 5-20 \text{ mm} \\ W &= 1-50 \text{ mm} \\ t_f &= 0.4-5 \text{ mm} \\ t_c &= 0.4-5 \text{ mm} \end{aligned} \tag{21}$$

For every choice of the input parameters $(q_G, \dot{m}, p_{cool})$, the mass of the panel is minimized subject to the constraints of section 3. The quadratic optimizer FMINCON, included in the package MATLAB®, was used; multiple random guesses were used to assure accurate solutions. When the optimizer failed to find a solution for a given choice of the input parameters, it was assumed that no solution existed for that particular parameter combination, resulting in a point outside the design space. The results can be summarized in the design map of Fig. 4. The lines separate parameter combinations that allow a feasible solution (inside the bell-shaped curve) from unacceptable

choices of parameters (outside the curve). For any value of coolant flow rate and internal pressure, Fig. 4 shows the maximum heat flux that can be imparted to the structure without violating any of the constraints. As every point in the map contains the result of an optimization process, very large amount of information is contained in this figure. Here we try to convey the major conclusions:

(i) At any given coolant pressure, there exists an optimal flow rate, $\dot{m}_{opt} \approx 3$ kg/s, resulting in the maximum possible heat flux. This optimal flow rate is essentially independent on the coolant pressure.

(ii) An increase in coolant pressure is beneficial; that is, higher heat fluxes can be safely tolerated at larger coolant pressures.

To rationalize these conclusions, it is necessary to analyze the optimization results in more detail. Every constraint can be associated to an activity parameter, Π: a value $\Pi = 1$ implies that the constraint is active (and thus deign-limiting). Fig. 5 shows the constraint activity parameters for the optimal geometries relative to a heat flux, $q_G = 3$ MW/m^2. Notice that at flow rates lower than $\dot{m}_{\min} \approx 0.5$ kg/s, no geometry can satisfy all the constraints. Since the only active constraint at $\dot{m}_{\min}$ is the resistance to the thermo-mechanical loads (for all the three values of p_{cool}), we can conclude that for $\dot{m} < \dot{m}_{\min}$ the cooling effect is not sufficient to maintain the stresses below the yield point of the material. As the flow rate increases, the pressure drop constraint eventually becomes active (and remains such afterwards). Notice that this event is retarded with increasing coolant pressure. This is easily explained using the equation of state (Eq. (22)). An increase in the gas pressure implies a proportional increase in its density; since the mass flow rate is kept constant, this must imply that the coolant slows down. The pressure drop has a quadratic dependence on the coolant velocity (Eq. (19)), resulting in a substantial advantage. This is responsible for the larger design space obtained at higher coolant pressures (Fig. 4).

It is interesting to look at the optimal dimensions of the structures as a function of the flow rate (and the coolant pressure). Fig. 6 shows the variation of the optimal height (*L*) and width (*w*) of the channels. Notice that at low flow rates, the height of the channel assumes its minimum allowable value (5 mm). After the pressure drop constraint becomes active, *L* increases to compensate for the increase in flow rate (Eq. (19)). The width of the channel, *w*, also increases, but a much lower rate: this is due to the fact that the width of the channel largely controls the bending stress in the face sheet members (Eq. (14)). Fig. 6 clearly shows the advantage of a large coolant pressure: since the coolant is slower at large p_{cool}, the hydraulic diameter (and hence *L* and *w*) can be lower without violating the pressure drop constraint, resulting in stress mitigation. The thicknesses of the face sheet and core members almost always assume their minimum allowable value (0.4 mm), and hence are not plotted (the exception is the face sheet thickness for $p_{cool} = 30$ MPa, which slightly increases at large flow rates).

As the flow rate is increased, eventually the opposing requirements on the panel geometry imposed by the pressure drop and the stress constraints result in impossible solutions.

In this study, it has been shown that an increase in the coolant pressure up to 30 MPa is beneficial, both at low and high flow rates. This trend is not expected to hold at arbitrary large coolant pressures. As the coolant pressure increases, the mechanical loads become proportionally more severe (Fig. 6). At $p_{cool} = 30$ MPa, the constraint associated with the resistance to the mechanical loads is active for most flow rates. If the pressure is increased well over 30 MPa, the resistance of the structure is likely to become a concern. Future work is needed to explore this regime, and identify the optimal coolant pressure.

5. CONCLUSIONS AND FUTURE WORK

Actively cooled metallic structures made of the Nickel superalloy MAR-M246 are proven to be effective as combustor walls for hypersonic vehicles over a large range of thermo-mechanical loads ($q_G = 1 - 6$ MW/m^2 and $p_{cool} = 5 - 30$ MPa). Although the actual loads in service conditions depend on a number of factors (e.g. the nature of the mission, the size and shape of the vehicle, the dynamic pressure), this range should encompass the low-to-moderate Mach number flight conditions for H_2-powered hypersonic vehicles (Mach 7-12) [18-22]. The design space for the combination of parameters (coolant flow rate, heat flux and coolant pressure) has been presented. An optimal flow rate, $\dot{m} \approx 3$ kg/s, has clearly emerged, independent on the coolant pressure. Somewhat surprisingly, the pressure in the cooling channels has a beneficial effect on the design space; that is, increasing the pressure from 5 to 30 MPa results in (i) higher acceptable heat flux and (ii) larger range of allowable flow rates. This trend is expected to reverse at higher pressures, when the mechanical resistance of the structure becomes a concern.

Future work includes the extension of these results to a larger range of parameters, the study of the effect of the coolant temperature at the inlet, and the exploration of different metallic materials. Also, a formal derivation of the thermo-mechanical loads as a function of the vehicle Mach number is underway.

ACKNOWLEDGMENTS

This work was supported by the ONR through a MURI program on Revolutionary Materials for Hypersonic Flight (Contract No. N00014-05-1-0439). The authors are thankful to David Marshall of Teledyne, and Thomas A. Jackson and William M. Roquemore of AFRL for insightful discussions.

REFERENCES

1. Valdevit, L., Vermaak, N., Zok, F. W., Evans, A. G., *Optimal design of actively cooled panels for scramjets.* AIAA Journal, Submitted, 2007.

2. Valdevit, L., Vermaak, N., Zok, F. W., Evans, A. G., *The effect of Mach number on materials selection for hypersonic vehicle design.* In preparation, 2007.
3. Lu, T.J., L. Valdevit, and A.G. Evans, *Active cooling by metallic sandwich structures with periodic cores*. Progress in Materials Science, 2005. **50**(7): p. 789-815.
4. Valdevit, L., et al., *Optimal active cooling performance of metallic sandwich panels with prismatic cores.* International Journal of Heat and Mass Transfer, 2006. **49**(21-22): p. 3819-3830.
5. Bejan, A., *Convection heat transfer*. 3rd ed. 2004, Hoboken, N.J.: Wiley. xxxi, 694.
6. Gnielinski, V., *New Equations for Heat and Mass-Transfer in Turbulent Pipe and Channel Flow.* International Chemical Engineering, 1976. **16**(2): p. 359-368.
7. Moody, L.F., *Friction factors for pipe flow.* Trans. ASME, 1944. **66**: p. 671-684.
8. Rathbun, H.J., F.W. Zok, and A.G. Evans, *Strength optimization of metallic sandwich panels subject to bending.* International Journal of Solids and Structures, 2005. **42**(26): p. 6643-6661.
9. Valdevit, L., J.W. Hutchinson, and A.G. Evans, *Structurally optimized sandwich panels with prismatic cores.* International Journal of Solids and Structures, 2004. **41**(18-19): p. 5105-5124.
10. Valdevit, L., et al., *Structural performance of near-optimal sandwich panels with corrugated cores*. International Journal of Solids and Structures, 2006. **43**(16): p. 4888-4905.
11. Wei, Z., F.W. Zok, and A.G. Evans, *Design of sandwich panels with prismatic cores.* Journal of Engineering Materials and Technology - Trans. of the ASME, 2006. **128**(2): p. 186-192.
12. Wicks, N. and J.W. Hutchinson, *Optimal truss plates*. International Journal of Solids and Structures, 2001. **38**(30-31): p. 5165-5183.
13. Wicks, N. and J.W. Hutchinson, *Performance of sandwich plates with truss cores.* Mechanics of Materials, 2004. **36**(8): p. 739-751.
14. Zok, F.W., et al., *Structural performance of metallic sandwich panels with square honeycomb cores*. Philosophical Magazine, 2005. **85**(26-27): p. 3207-3234.
15. Zok, F.W., et al., *Design of metallic textile core sandwich panels.* International Journal of Solids and Structures, 2003. **40**(21): p. 5707-5722.
16. Zok, F.W., et al., *A protocol for characterizing the structural performance of metallic sandwich panels: application to pyramidal truss cores.* International Journal of Solids and Structures, 2004. **41**(22-23): p. 6249-6271.
17. Boley, B.A. and J.H. Weiner, *Theory of thermal stresses*. 1960, New York: Wiley.
18. Heiser, W.H. and D.T. Pratt, *Hypersonic airbreathing propulsion*.1994, Washington: AIAA.
19. Walters, F.M. and O.A. Buchmann, *Heat transfer and fluid flow analysis of Hydrogen-cooled panels and manifold systems*, NASA CR-66925.
20. Youn, B. and A. F. Mills, *Cooling panel optimization for the active cooling system of a hypersonic aircraft*, Journal of Thermophysics and Heat Transfer, 1995. **9**(1): p.136-143.
21. Buchmann, O.A., *Thermal-structural design study of an airframe-integrated scramjet*, 1979. NASA CR-3141.
22. D. Marshall, personal communications.

APPENDIX 1

THE PHYSICAL PROPERTIES OF HYDROGEN

Hydrogen is a highly compressible gas, and as a result, many of the properties change significantly over the relevant range of temperatures (and pressures). For large heat fluxes and low flow rates, the temperature increase in the coolant over a 1m-long panel can be as large as 600K (Eq.(4)). Over this range, we need to account for properties variation. Since the specific heat of hydrogen doesn't vary considerably over the range T = 50-1000K, we assume it constant and equal to $c_p = 14,600$ J/kg K. Similarly, we ignore variations in the Prandtl number and assume Pr=0.68. Density is assumed to vary with coolant pressure and temperature, whereas viscosity and thermal conductivity vary with temperature only.

Density

For temperatures lower than 1000K (the range of interest for active cooling, since injection typically occurs at temperature lower than or roughly equal to 1000K), H_2 can be modeled as an ideal gas. It follow that the density is a function of temperature and pressure according to:

$$\rho = \frac{p_{cool}}{RT} \qquad (22)$$

where R is the gas constant for H_2 (Table 2).
It is legitimate to ignore the pressure drop over the channels, and treat the pressure as uniform. Consequently, the density changes uniquely as a function of the temperature. As the fluid gets hotter, its density decreases. Since the mass flow rate of H_2 is constant (by continuity), it follows that the volumetric flow rate (and the velocity in the ducts) increases towards the end of the channels.

Dynamic viscosity

The variation of the dynamic viscosity with temperature can be modeled with Sutherland's formula:

$$\mu = \mu_0 \frac{T_0 + C_\mu}{T + C_\mu}\left(\frac{T}{T_0}\right)^{3/2}$$

where the parameters for hydrogen are given in Table 2.
The dynamic viscosity is not significantly affected by pressure.

Thermal conductivity

The thermal conductivity is fairly unaffected by pressure, but shows some temperature sensitivity. A Sutherland temperature dependence can be assumed:

$$k = k_0 \frac{T_0 + C_k}{T + C_k} \left(\frac{T}{T_0} \right)^{3/2}$$

where the parameters for hydrogen are given in Table 2.

Note that these formula are typically valid for temperatures lower than 600K; we speculate that the error won't be too large in the range 600K<T<1000K.

TABLES

Table 1 – Materials properties for the nickel superalloy, MAR-M246

Property	ρ_s [kg/m^3]	k_s [W/mK]	E [GPa]	α_s [10^{-6}/K]	ν_s	σ_{Y0} [MPa]	$\mathrm{d}\sigma_Y / \mathrm{d}t$ [MPa/K]	T^* [K]
Value	8440	25.94	161	16.7	0.3	800	-0.564	1089

Table 2 – Physical properties of hydrogen (specific heat and Prandtl number are assumed temperature-independent for simplicity)

Property	c_p [J/kgK]	Pr	R [J/kgK]	μ_0 [Pa·s]	T_0^μ [K]	C_μ [K]	k_0 [W/mK]	T_0^k [K]	C_k [K]
Value	14,600	0.68	4,016	$0.876 \cdot 10^{-5}$	293	27	0.162	250	110

FIGURES

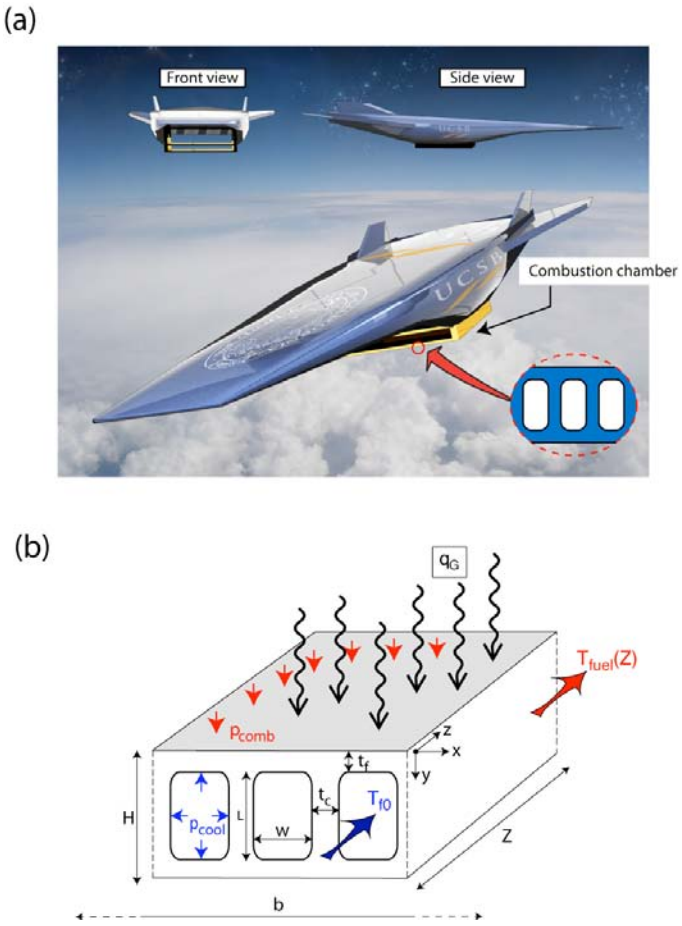

Figure 1 – (a) Artist rendition of a hypersonic air-breathing vehicle. The proposed multifunctional actively cooled plate is shown in the inset. (b) Schematic of the actively cooled plate with thermo-mechanical loads, variables definition and coordinate system.

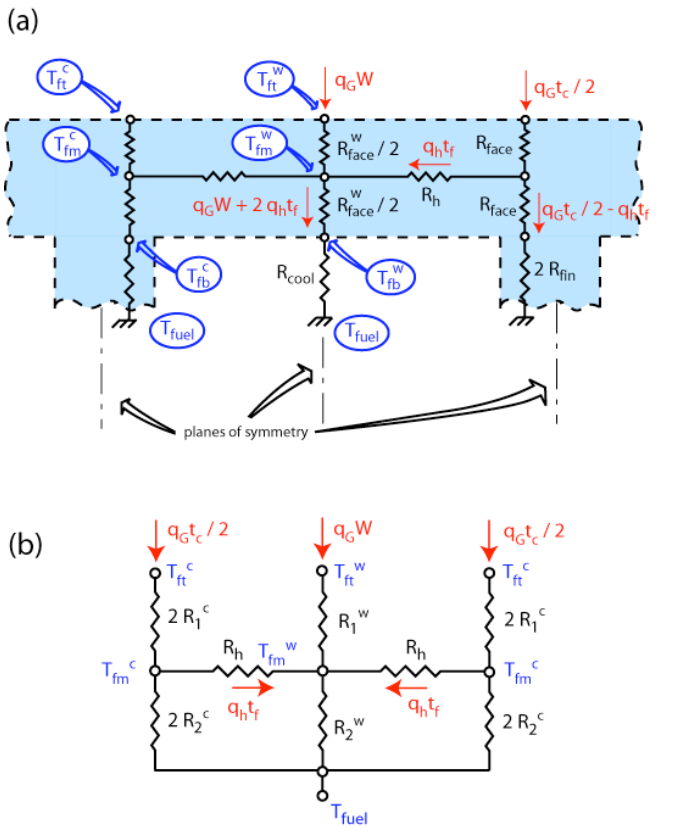

Figure 2 – (a) Thermal resistance network used for the temperature calculations. (b) Effective network.

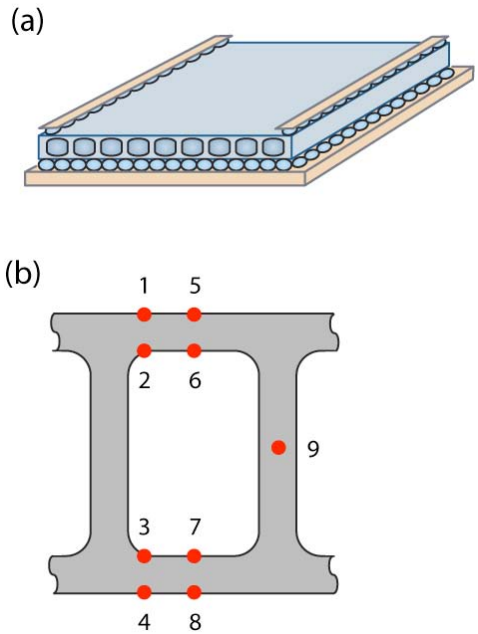

Figure 3 – (a) Boundary conditions used for the thermo-mechanical stress calculations. (b) The critical points considered for failure at any given cross-section.

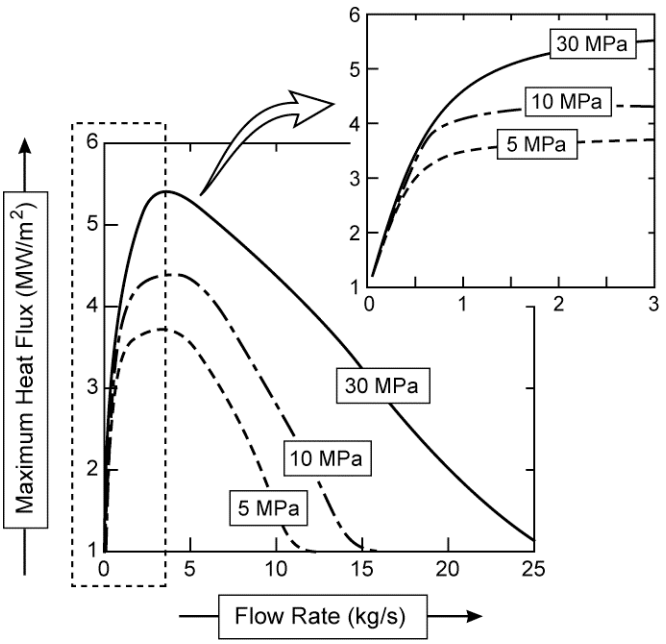

Figure 4 – Design map for the Nickel superalloy MAR-M216 for 3 different values of coolant pressure. Notice how increasing the coolant pressure significantly expands the design space. The inset shows the most relevant portion of the map.

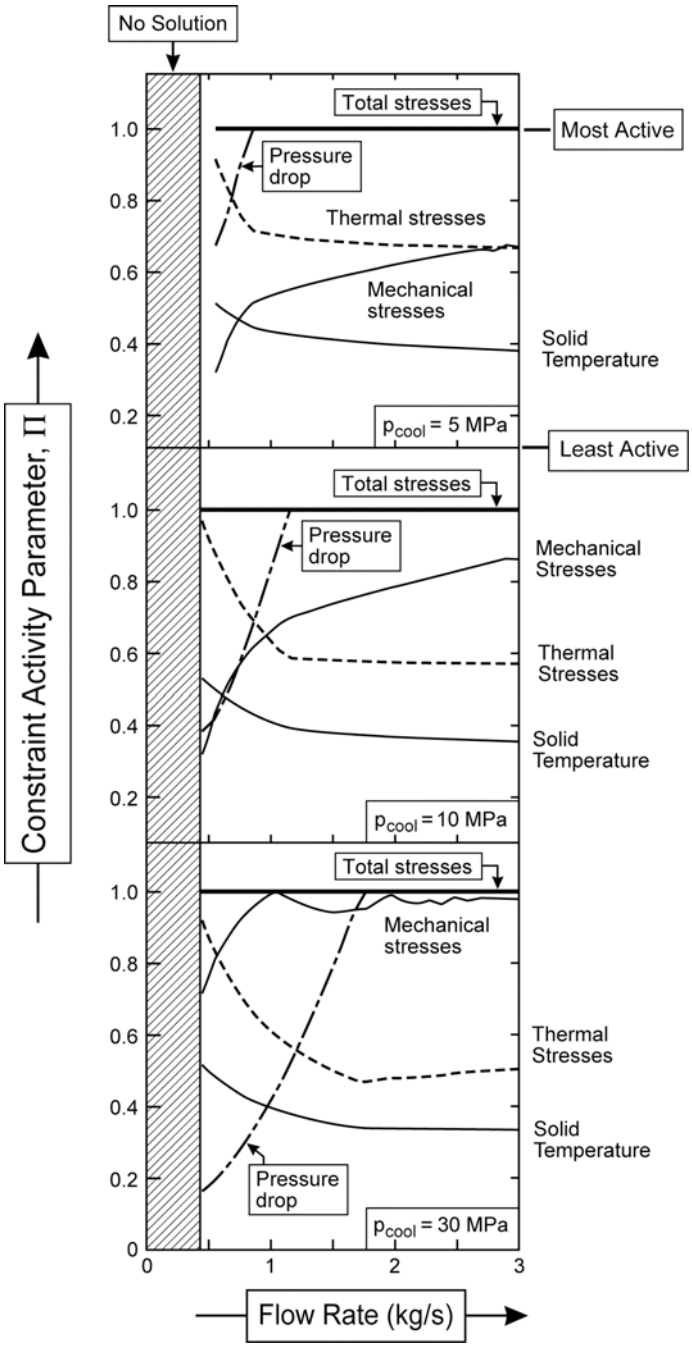

Figure 5 – Constraint activity parameters, Π for optimal designs at a prescribed heat flux, $q_G = 3\ \mathrm{MW/m^2}$. A parameter $\Pi = 1$ indicates that the constraint is active (and thus design-limiting).

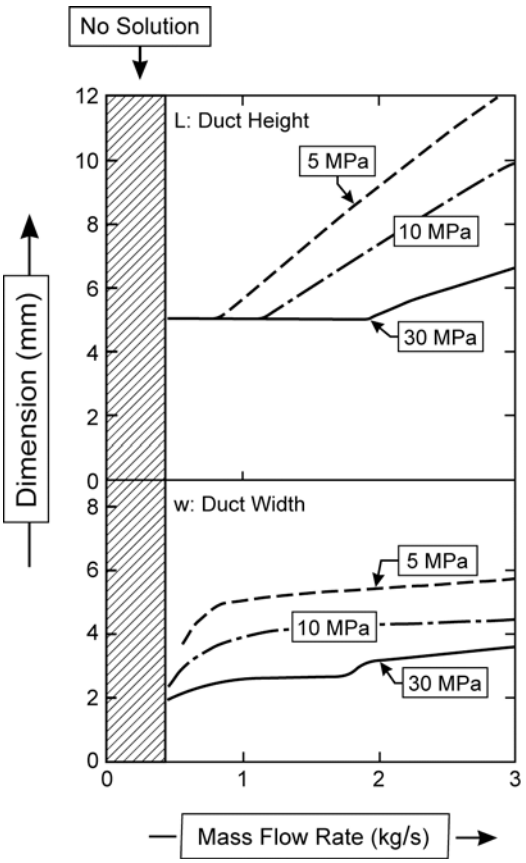

Figure 6 – Optimal dimensions for the panels optimized for a prescribed heat flux, $q_G = 3\ \mathrm{MW/m^2}$. The other two dimensions (face sheet thickness, t_f, and core web thicknesses, t_c, always assume the minimum value of 0.4 mm (the exception is t_f for the case $p_{cool} = 30\ \mathrm{MPa}$, which increases slightly at large flow rates).